

A STUDY TO COMPARING SPHERICAL, ELLIPSE AND FLAT FORMING TOOL PROFILE EFFECT IN SINGLE POINT INCREMENTAL FORMING BY FINITE ELEMENT ANALYSIS

Khalil Ibrahim ABASS ^{1,2}

The Single Point Incremental Forming Process (SPIF) is a forming technique of sheet material based on layered manufacturing principles. The description of the process is more complicated by highly nonlinear boundary conditions. The paper presents a study of effect (spherical, ellipse and flat) forming tool profile on SPIF through FEA, that permits the modeling of complex geometries, material behavior and boundary conditions. The results showed that the model of simulation can predict an ideal profile of processing track, spring back error of SPIF and the behavior of contact tool-workpiece, also on the accuracy of product.

Keywords: forming tool, single point incremental forming (SPIF), finite element analysis (FEA).

1. Introduction

Incremental sheet metal forming (ISMF) is a new innovative combination of computer technology with machine, and this makes it a flexible process. The geometry of the product is included into two-dimensional layers and the designed shape is deformed in multilayer using CNC controlled movement of a hemispherical forming tool [1]. Single point incremental forming (SPIF) is a flexible sheet metal forming process with potential for small production and for rapid dies. A forming tool, moving along a 3D profile at a constant depth increment in vertical direction, gradually deforms the blank into a designed product (Fig. 1, [2]). The tool path is programmed by computer aided manufacturing (CAM) software and used in an NC milling machine for execution.

¹ University POLITEHNICA of Bucharest, Bucharest, Romania, khalil1969a@yahoo.com

² The University of Mustansiriyah, Baghdad, Iraq

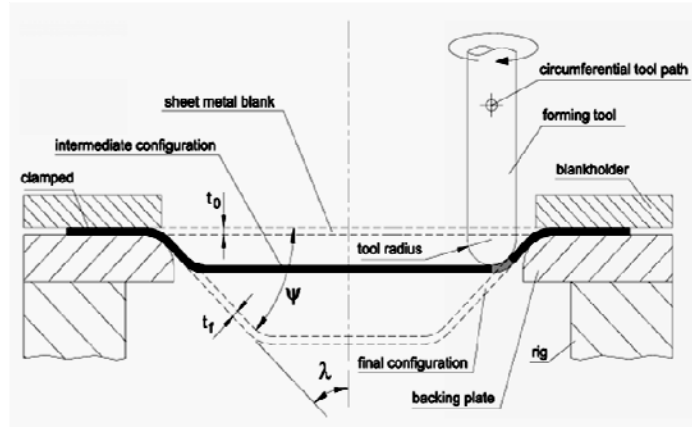


Fig. 1. SPIF Technology where: initial thickness (t_o), final thickness (t_f), wall angle (λ) [2]

The SPIF process presents some disadvantages: longer forming time compared to Deep Drawing Process, it only allows small production batches, lower geometry accuracy, higher springback, especially in convex radius and bending edges areas [3].

The main process parameters that influence the accuracy and the surface quality of the formed part are: tool diameter (D_p), spindle speed (ω), feed rate (v) and tool vertical step down (Δz). Good quality parts can be produced by selecting the optimal parameters and the tool path trajectory [4].

The advantages of the SPIF process are: high process flexibility, low hardware costs, enhanced formability, enabling production of complex shapes without die sets, lower time-to-market. SPIF would be useful for prototyping and small-lot production for automobile, aerospace and biomedical industries [5].

In SPIF, the deformation of the sheet only occurs in the processing zone and is a combination of stretching and shearing. As a result, sheet thinning occurs during Single point incremental forming process. The final wall thickness (i.e. after thinning) is lower than the original blank sheet thickness especially under uni-axial deformation [6].

2. Literature Review

Many researchers used wide range, between 2 and 25 mm of round head to study the effect of forming tool radius value on the accuracy, force and ability of deforming in the SPIF process.

M. Ham and J. Jeswiet (2006) [7] researched the interaction between the material thickness and tool size. They concluded that the maximum forming angle is influenced by this interaction.

G. Hussain and et al. (2010) [8] investigated the formability of AA-2024 sheets. The operating parameters with wide ranges that were studied were forming tool radius, step size, and speed of forming of SPIF process. The effect on the formability was observed through a response surface method called central composite rotational design. The paper concludes that step size and tool radius have an important effect on the formability. The formability, depending on the forming tool radius, can decrease or increase with increasing the step size. The authors recommend to rationally choosing the combination of these parameters to increase the sheet formability.

M. B. Silva and et al. (2011) [9] used in the experiment five hemispherical head forming tools with 4 to 25 mm radius to deform aluminum AA1050-H111. The results show that, for the small tool radius, the stability effect is not significant to ensure localization, and the failure mechanism will change to promote fracture with suppression of necking. For large tool radius, the stability effect is able to raise the forming limit curve above the common limit curve of the stamping process to ensure localization by necking.

Some researchers studied other types of forming tool, such as flat surface at the bottom with radius value at the edge and showed effect on stress and strain distributions and on product quality. Xu Ziran and et al. (2010) [10] used two kinds of tools - with flat and hemispherical heads. It was found that the flat head tools can provide better profile accuracy and formability than the hemispherical head tools. Also, flat head tools required lower forming force than the hemispherical head tools.

A lot of researchers didn't take into account the effect of the forming tool diameter and selected one type or one value, depending upon previous papers as, B. T. Araghi and C. Robert [11, 12] who selected a 30 mm tool diameter, or M. Fiorotto [13], A. K. Behera [14] and C. F. Guzmán [15] who selected a 10 mm tool diameter.

P. Eyckens and et al. (2011) [16] selected a 5 to 10 mm tool diameter to predict tool diameter effect and step size with low rotating speed by FEM. T. A. Marques and et al. (2012) [17] selected tool diameter between 8 and 12 mm to investigate the tool diameter effect on polymer products.

This research focuses on using a new type of forming tool shape profile (ellipse) and on evaluating the product profile, thickness, strain and stress distribution after usage, compared to other tool profiles (hemispherical and flat). A new type of evaluation was used - chattering and contact status to observe the behaviour of the entire blank surface and not only the surface which was in contact with the forming tool.

3. Development of a FE Model

In developing the FE model it was endeavored to closely represent the real forming process. In this study, a general purpose of linear and nonlinear FEM analysis program, ANSYS 11, is used. Command script files, also called procedure files, were used to improve some tedious data input tasks during pre- and post-processing, by entering the FEM in a system for an integrated engineering approach to sheet metal forming. A flow diagram (Fig. 2) illustrates such an integrated system. The input stage includes model geometric, material properties and boundary conditions. The processing stage includes strain analysis by finite element method and computed shape, for the product success or failure. The output stage includes complete product for evaluation and conclusions.

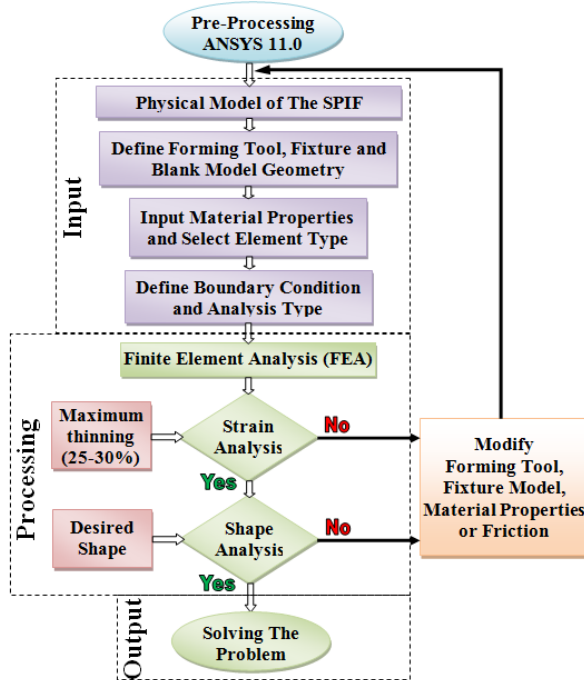


Fig. 2. Simulation flowchart illustrating input conditions, processing and output results

An FE model of SPIF process simulation was developed. The model includes the effect of contact between the tool set (forming tool, die and blank holder) and workpiece, as well as the elastic-plastic material behavior of the workpiece. To develop the FE model, the effect of spherical, ellipse and flat head forming tools was studied with constant values (dimension and materials) of forming tool, fixture and blank, as shown in Table 1.

Symmetric elements are used to model blanks that are rotationally symmetric about an axis. In this case, the deformed blanks are subjected to the loads from the forming tool and supporting die. A two dimensional analysis of a sector of the deforming blank is carried out in order to yield the complete stress and strain distributions. The actual components necessary for SPIF operation are shown in Fig. 1 to simulation in a FE model.

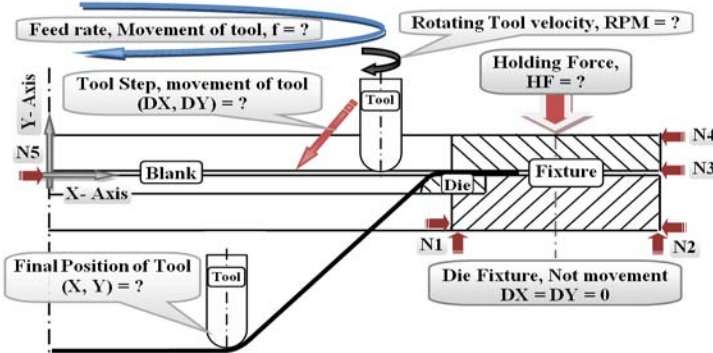


Fig. 3. Force and displacement boundary conditions of the SPIF process

The element V15C0106-2D was chosen to represent the workpiece and the element PLANE42-2D to represent the tool set (forming tool, die and blank holder) and both have translations in the nodal X and Y directions. A pure Al AA1050 was used, with the specific mechanical properties resulted from Stress-Strain curve of a tensile test (Table 1).

Table 1

Material properties of the blank

Variable	Value
Density, ρ	2700
Young's modulus, E	75
Poisson's ratio, ν	0.3
Yield stress, σ_y	80
Tangent modulus, E_t	0.5
Dia. of active Forming Tool, D_p	10 (mm)
Radius of Die, D_d	5 (mm)
Blank Thickness, t	0.9 (mm)
Step Size, z	0.2 (mm)
Dia. of Blank, D_b	226 (mm)
The friction coefficient, μ	0.05

A quadrilateral mapped mesh is used for blank. The boundary conditions (displacement, loading and the contact) are represented by following (Fig. 3):

1. A zero displacement constraint in the direction x is imposed at nodes along the workpiece centerline, N5;
2. The die was held fixed by nodal constraints in the direction x and y, N1 and N2;
3. The blank holder was constrained so as to allow only movement in the direction y, N3 and N4;
4. The forming tool motion was specified in profile with constant speed (Fig. 4).

Three contact interfaces were defined in the model:

- A. forming tool/upper blank surface interface,
- B. lower blank surface/die interface,
- C. blank holder/upper blank surface interface.

The elements used to represent the contact between the workpiece and the tool set, which include the forming tool, die and blank holder are CONTAC169 and CONTAC171-2D Point-to-Surface Contact, like a Rigid-to-flexible contact. The real constant set was used for each contact surface. A non-linear analysis, convergence criteria, incremental load and specified load steps are applied. The convergence tolerance was based on minimization of the force residual. The default tolerance in ANSYS is 10%.

5. Results and Discussion

The good prediction that results from simulation model depends on some factors such as:

1. Practical study of forming process using real conditions in order to fully understand the variables - single variables (movement in x and y direction) and combination variables (the friction coefficient feed rate).
2. Design and build a mathematical model for the simulation that is based upon the actual practical foundations of the forming process, which includes entering maximum number of variables in simulation model.
3. Using prediction tools such as thickness, strain and stress distributions, as well as forces measurements and comparing of the figures.

Evaluation of the results was depending upon the following:

1. Analysis of the forming tool movement from Auto CAD application.
2. Studying the resulting product shape (profile) from simulation depending upon forming tool movement.
3. Comparing of thickness, stress, strain and contact area distributions.
4. Evaluating of chattering states at tool/workpiece interface.

In Fig. 4, forming tool movement by 45° at three stages (2x2, 23.5x23.5, 47x47) mm in x and y directions, we can see contact the distance for three types of forming tool profile (spherical, ellipse and flat). Both spherical and ellipse forming tools start contact with a point and by increasing of depth (in the end of stroke), the shape of the blank surface will be identical to the forming tool shape.

Maximum contact distance was 3.24, 4.74 mm respectively. The flat forming tool starts with line then it curves the shape like the forming tool shape with increasing depth. Depth of deforming was 6.136 mm. Also all of them will have increased contact area with increased depth of deforming. At the same time, the end edge of product changes to much the shape of the forming tool profile.

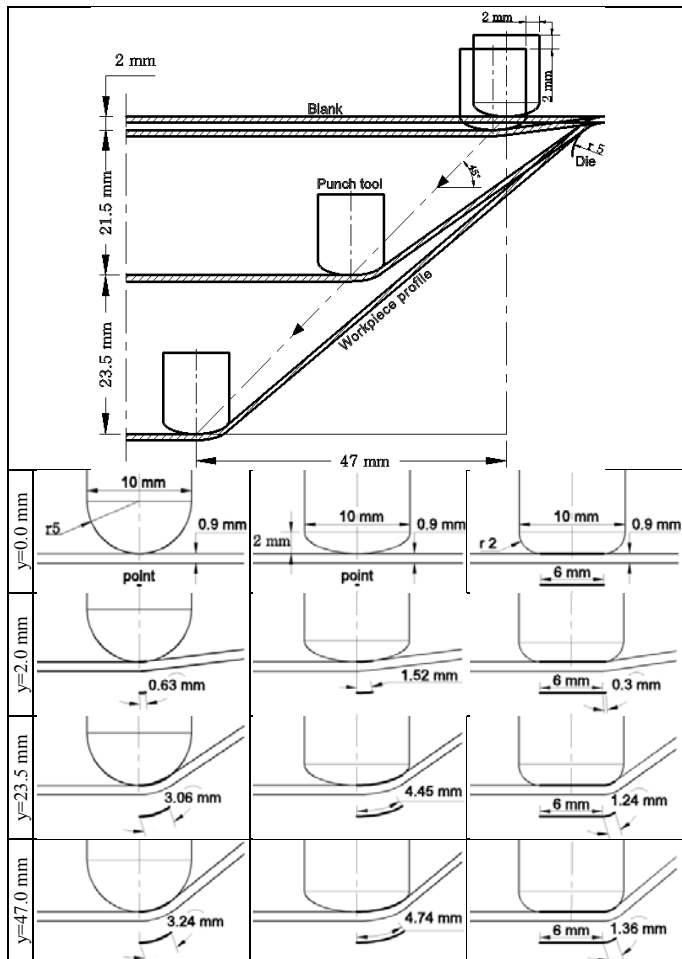


Fig. 4. Forming tool profile movement and a comparing of contact areas of spherical, ellipse and flat

The contact behavior prediction of the three types of forming tools and product surface (Fig. 5) is different from the contact behavior in AutoCAD prediction. According to this prediction were identified four regions (sticking, sliding, near contact and far open) that are different by figure and contact area depending upon depth of deformation.

The flat region of the flat forming tool is always far from contact with product surface. That means the contact area is small and the real contact is only on the curve of the forming tool edge that is influenced by revolving speed and the active diameter of forming tool. The contact behavior of spherical and ellipse forming tools are influenced by the deformed metal behavior which suffers from springback, causing increased contact region area, also increased friction and plastic region, which suffer from sticking.

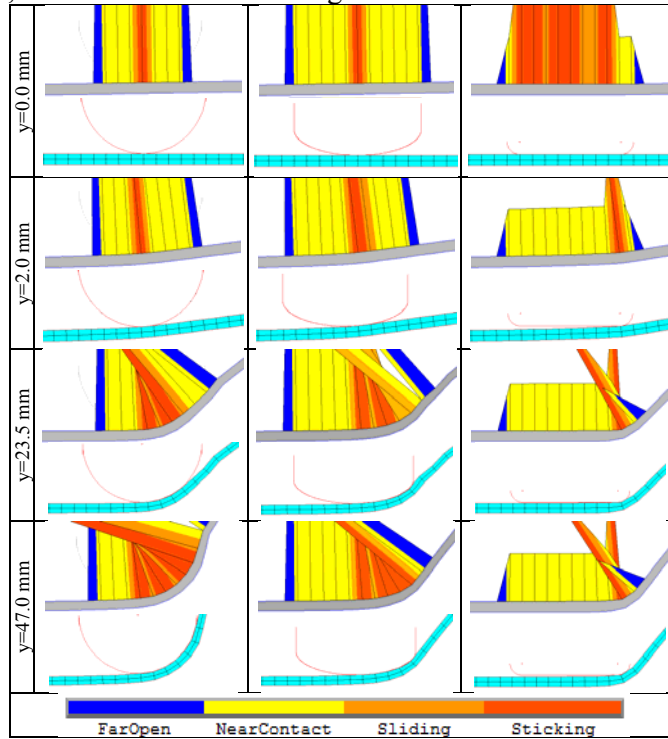


Fig. 5. Forming tool profile structure and contact status of spherical, ellipse and flat forming tool profiles

The revolving forming tool around its axis, the constant rate of movement along the contour of the product and the support-free wide blank area produce a forming operation similar to "continuous deforming with pulses". This operation will produce a continuous vibration of the blank. The level of vibration is also affected by depth of deformation and product shape. Large support-free area and increased vibration lead to the appearance of chattering effect as shown in Fig. 6.

This chattering state is influenced by the contact area, its occurrence being larger when using flat forming tool as shown in the ideal Auto CAD predictions that propose non-springback and non-metal plastic. Fig. 7 shows the results when the contact area of the forming tool is spherical, ellipse and flat. The plastic

deformation of metal and the springback increase proportionally with deformation depth, especially in the case of the spherical forming tool.

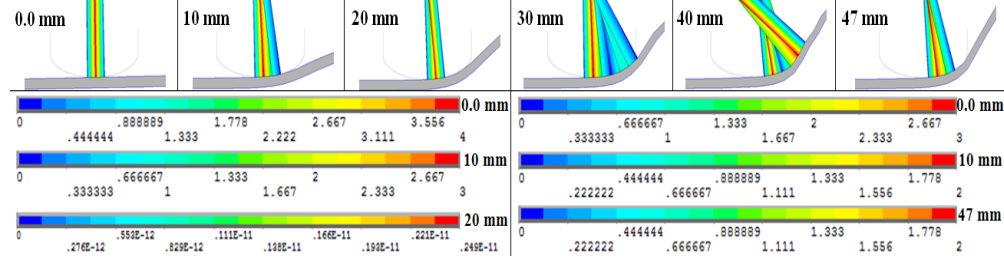


Fig. 6. The ellipse forming tool profile movement and deformed blank profiles

Successive stages of the deformed sheet by FEM simulation of SPIF process and forming tool strokes are shown in Fig. 7. The results represent the forming stages of three types of forming tools (ellipse, spherical and flat):

1. The shape of the hollow-end of the product was similar to the shape of the forming tool.
2. The springback was very clear with changing forming tool profile and the predicted shape was very different with spherical head (Fig. 4).

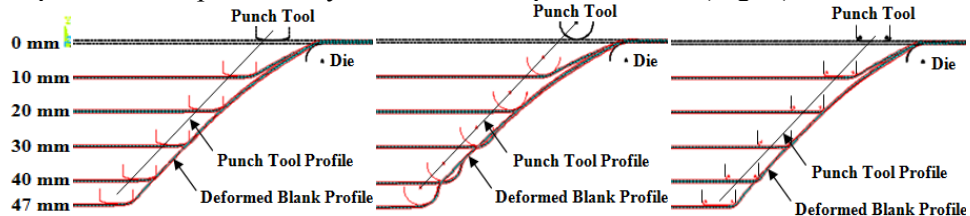


Fig. 7. Forming tool profile movement and deformed blank profiles of Ellipse, Spherical and Flat

Thickness distribution and strain field across the formed part are necessary to any intermediate formability evaluation. In this section it was determined the thickness variation and localized strain across the formed part. Fig. 8 shows the effect of the forming tool profile on the thickness distributions of the cup for a 47 mm forming tool stroke when the part is completely drawn.

The largest thinning values for all cups happened at 41.3 mm depth and 40 mm distance from the center of the cup. The maximum thinning occurred for spherical forming tool profile, due to sever metal bending. In the area where high reduction in thickness for spherical forming tool happens, a neck results, indicating failure of the product at this stage. The changing in thickness distribution are the result of the forming tool profile changing.

Strain distribution that results from simulation model represents strain value for each node in numerical mode of SPIF and also strain values of all nodes at each step size of forming tool. That means huge number of results. And Fig. 9 represents the effect of forming tool profile on strain distribution at upper surface

of workpiece, for forming tool stroke at 47 mm depth and 45° angle, i.e., when the part is completely drawn and removed from the die.

It is also concluded that the peak values of strains are concentrated between 40 to 60 mm distance from the center of cup and 19.5 to 42.2 mm depth and they decrease toward the cup center. This means that the maximum values of strain will be concentrated on the places where the forming tool touches and moves. No forming operation occurs under blank holder, the strain distribution is more uniform and the strain values were reasonable at 0 to 40 and 60 to 90 mm distance from center of cup.

The distributions of upper surface strain of the flat forming tool was more uniform and had more reasonable values than the ellipse forming tool.

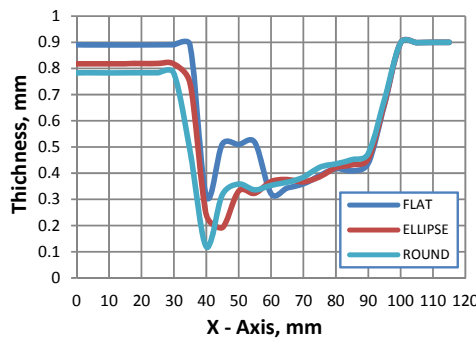


Fig. 8. Thick Distribution of forming tool (spherical, ellipse and flat)

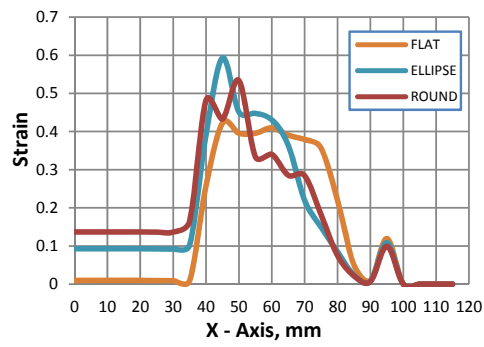


Fig. 9. Strain distribution of forming tool (spherical, ellipse and flat)

Successive stages of the SPIF sheet for ellipse forming tool profile are shown in Fig. 10. It is clear that the forming tool stroke influences greatly the stress values, in which these values increase with stroke. It is seen from the figures that stress peaks are located at the contact places between forming tool profile and workpiece. The peak height appears to be a good indicator to assess whether a forming operation will be successful or not. The figures show how severe the stress distribution located at the end of stroke (at the corner of the product) is and the occurrence of a localized neck is obvious. Fracture was observed along a sharp corner. This was predicted by a high value of the stress.

The figure also shows the successive stages at 2, 5, 15, 25, 35 and 47 mm in depth of contact statuses distributions until the final product. The followings can be observed:

- The increase of contact effects with increase contact area and depth of deformation until maximum contact area at end of stroke.

- Increasing and translating sticking region with increasing depth of deformation around the forming tool and hence increasing fracture probability because of repeated reforming in wide region, especially with spherical head.

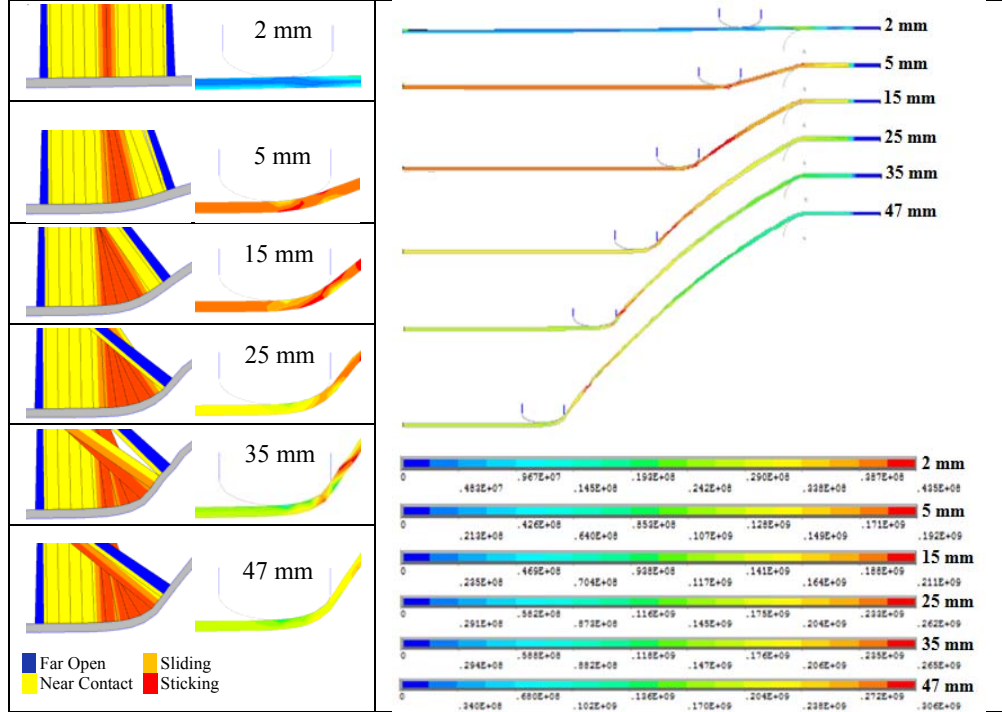


Fig. 10. Effect of the stress and the contact distribution stages of ellipse forming tool profile

6. Conclusions

The interaction of forming tool profile and sheet thickness distributions plays an important role in the generation and forming of defects. For a given sheet thickness, a changing in the forming tool profile can be helpful in inhibiting the formation of wall and corner fold around forming tool.

It is demonstrated that any changing in forming tool profile has effect on the formability in SPIF depending on figure and area of the contact. In another words decrease of the contact area of forming tool not necessarily will improve the product accuracy.

The results showed that the simulation model can predict an ideal profile of processing track and the springback error of SPIF is effectively eliminated. The use of proper simulation system (prediction model) and high accuracy procedure can allow high level of prediction.

Trial and error in traditional SPIF can be reduced and the workpiece dimensional accuracy can be greatly improve Increasing of the references and indications by FEM can give an accurate prediction of the deforming behavior.

R E F E R E N C E S

- [1]. *R.P.Singh, G.Goyal*, “FEA analysis to study the influence of various forming parameters on springback occurs in single point incremental forming”, Int. J. Eng. Research and Applications (IJERA) ISSN: 2248-9622, (AET-2014), pp. 33-37.
- [2]. *M.B.Silva, M.Skjødt, A.G Atkins, N.Bay, P.A.F.Martins*, “Single-point incremental forming and formability-failure diagrams”, J. Strain Analysis for Eng. Design, **vol. 43**, 1, 2008, pp. 15-35.
- [3]. *R.Benmessaoud*, “A Tool path generation method for the multi-pass incremental forming process investigation”, Int. J. Adv. Research in Computer Sci. and Soft. Eng., **vol. 4**, 5, 2014, pp. 1035-1044.
- [4]. *R.CRINA*, “new configurations of the spif process-a review”, “Vasile Alecsandri” University of Bacau, Romania, J. of Eng. Studies and Research, **vol. 16**, 4, 2010, pp. 33-39.
- [5]. *M.A.Dittrich, T.G.Gutowski, J.Cao, J.T.Roth*, “Exergy analysis of incremental sheet forming”, J. Production Engineering, **vol. 6**, 2, 2012, pp. 169-177.
- [6]. *G.Hussain, N.Hayat, G.Lin*, “Pyramid as test geometry to evaluate formability in incremental forming: Recent results”, J. Mech. Sci. and Tech., **vol. 26**, 8, 2012, pp. 2337-2345.
- [7]. *M.Ham, J.Jeswiet*, “Single Point Incremental Forming and the Forming Criteria for AA3003”, CIRP Annals - Manufacturing Technology, **vol. 55**, 1, 2006, pp. 241-244.
- [8]. *G.Hussain, L.Gao, N.Hayat, N.U.Dar*, “The formability of annealed and pre-aged AA-2024 sheets in single-point incremental forming”, Int. J. Adv. Manuf. Technol. **vol. 46**, 5-8, 2010, pp. 543-549.
- [9]. *M.B.Silva, P.S.Nielsen, N.Bay, P.A.F.Martins*, “Failure mechanisms in single-point incremental forming of metals”, Int. J. Adv. Manuf. Technol. **vol. 56**, 9-12, 2011, pp. 893-903.
- [10]. *X.Ziran, L.Gao, G.Hussain, Z.Cui*, “The performance of flat end and hemispherical end tools in single-point incremental forming”, Int. J. Adv. Manuf. Technol., **vol. 46**, 9-12, 2010, pp. 1113-1118.
- [11]. *B.T.Arighi, G.L.Manco, M.Bambach*, “Investigation into a new hybrid forming process: Incremental sheet forming combined with stretch forming”, CIRP Annals - Manuf. Tech., **vol. 58**, 1, 2009, pp. 225-228.
- [12]. *C.Robert, A.Delameziere*, “Comparison between incremental deformation theory and flow rule to simulate sheet-metal forming processes”, J. Mate. Pro. Tech., **vol. 212**, 5, 2012, pp. 1123-1131.
- [13]. *M.Fiorotto, M.Sorgente, G.Lucchetta*, “preliminary studies on single point incremental forming for composite materials”, Int. J. Mater. Form., **vol. 3**, 1, 2010, pp. 951-954.
- [14]. *A.K.Bhera, J.Verbert, J.R.Duflou*, “Tool path compensation strategies for single point incremental sheet forming using multivariate adaptive regression splines”, Computer-Aided Design, **vol. 45**, 3, 2013, pp. 575-590.
- [15]. *C.F.Guzmán, J.Gu, J.Duflou*, “Study of the geometrical inaccuracy on a SPIF two-slope pyramid by finite element simulations”, Int. J. of Solids and Structures, **vol. 49**, 25, 2012, pp. 3594-3604.
- [16]. *P.Éyckens, B.Belkassem, C.Henrard*, “Strain evolution in the single point incremental forming process: digital image correlation measurement and finite element prediction”, Int. J. Mater. Form., **vol. 4**, 1, 2011, pp. 55-71.
- [17]. *T.A.Marques, M.B.Silva, P.A.F.Martins*, “On the potential of single point incremental forming of sheet polymer parts, Int. J. Adv. Manuf. Technol., **vol. 60**, 1-4, 2012, pp. 75-86.